Published in final edited form as:

Free Radic Biol Med. 2017 September ; 110: 54–62. doi:10.1016/j.freeradbiomed.2017.05.019.

Mesna (2-mercaptoethane sodium sulfonate) functions as a regulator of myeloperoxidase☆

Roohi Jeelani[a], **Seyedehameneh Jahanbakhsh**[a], **Hamid-Reza Kohan-Ghadr**[a], **Mili Thakur**[a], **Sana Khan**[a], **Sarah R. Aldhaheri**[a], **Zhe Yang**[b], **Peter Andreana**[c], **Robert Morris**[a,d], **Husam M. Abu-Soud**[a,b,*]

[a]Department of Obstetrics and Gynecology, Wayne State University School of Medicine, Detroit, MI, 48201, United States

[b]Department of Microbiology, Immunology and Biochemistry, Wayne State University School of Medicine, Detroit, MI, 48201, United States

[c]Department of Chemistry and Biochemistry and School of Green Chemistry and Engineering, University of Toledo, Toledo, OH 43606, United States

[d]Karmanos Cancer Institute, Detroit, MI, 48201, United States

Abstract

Myeloperoxidase (MPO), an abundant protein in neutrophils, monocytes, and macrophages, is thought to play a critical role in the pathogenesis of various disorders ranging from cardiovascular diseases to cancer. We show that mesna (2-mercaptoethanesulfonic acid sodium salt), a detoxifying agent, which inhibits side effects of oxazaphosphorine chemotherapy, functions as a potent inhibitor of MPO; modulating its catalytic activity and function. Using rapid kinetic methods, we examined the interactions of mesna with MPO compounds I and II and ferric forms in the presence and absence of chloride (Cl^-), the preferred substrate of MPO. Our results suggest that low mesna concentrations dramatically influenced the build-up, duration, and decay of steady-state levels of Compound I and Compound II, which is the rate-limiting intermediate in the classic peroxidase cycle. Whereas, higher mesna concentrations facilitate the porphyrin-to-adjacent amino acid electron transfer allowing the formation of an unstable transient intermediate, Compound I*, that displays a characteristic spectrum similar to Compound I. In the absence of plasma level of chloride, mesna not only accelerated the formation and decay of Compound II but also reduced its stability in a dose depend manner. Mesna competes with Cl^-, inhibiting MPO's chlorinating activity with an IC_{50} of 5 μM, and switches the reaction from a $2e^-$ to a $1e^-$ pathway allowing the enzyme to function only with catalase-like activity. A kinetic model which shows the dual regulation through which mesna interacts with MPO and regulates its downstream inflammatory pathways is presented further validating the repurposing of mesna as an anti-inflammatory drug.

*Corresponding author at: Department of Obstetrics and Gynecology, Wayne State University School of Medicine, The C.S. Mott Center for Human Growth and Development, Detroit, MI 48201, United States. habusoud@med.wayne.edu (H.M. Abu-Soud).

Author contributions

RJ and HA designed the study, coordinated the work and wrote the paper. RJ, SJ, HK, SA, SK and HA designed, performed and analyzed the experiments as reflected in the figures below. ZY designed, performed and designed the model in Fig. 10. HK, PA, MT and RM provided technical assistance and contributed to the preparation of the figures and help draft the paper. All authors reviewed the results and approved the final version of the manuscript.

None of the authors listed have any financial conflicts to disclose.

Keywords

Mesna; Halides; Inflammation; Mammalian peroxidases; Cancer; Stopped-flow; Kinetics; Chemotherapy

1. Introduction

Myeloperoxidase (MPO) is a dimeric hemoprotein with two identical subunits. Each subunit is comprised of light and heavy chains with molecular masses of 15 and 60 kDa, respectively [1,2]. MPO utilizes hydrogen peroxide (H_2O_2) as the electron acceptor in the catalysis of oxidative reactions, which have a critical role in the generation of inflammatory injury specifically in cardiovascular diseases [3–5]. Under physiological conditions, MPO catalyzes the formation of antimicrobial species such as cytotoxic hypochlorous acid (HOCl), through the oxidation of chloride (Cl^-) as the substrate [3,5]. Indeed, MPO is the only human enzyme known to selectively generate reactive chlorinating species under physiological concentration of halides [6]. MPO final products can serve as markers to identify sites of MPO-mediated oxidative damage [7–10]. The mechanism that governs the typical MPO catalytic activity is represented in Eq. (1)–(5):

$$\text{MPO-Fe(III)} + H_2O_2 \rightarrow \text{MPO-Fe(IV)} = O^{\bullet+}\pi_{\text{Por}} + H_2O \quad (1)$$

Compound I.

$$\text{Compound I} + Cl^- + H^+ \rightarrow \text{MPO-Fe(III)} + \text{HOCl} \quad (2)$$

$$\text{Compound I} + AH_2 \rightarrow \text{MPO-Fe(IV)} = O + {}^{\bullet}AH \quad (3)$$

Compound II.

$$\text{Compound I} \rightarrow \text{MPO-Fe(IV)} = O^{\bullet+}\pi\text{ami} \rightarrow \text{Compound II} \quad (4)$$

Compound I*.

$$\text{Compound II} + AH_2 \rightarrow \text{MPO-Fe(III)} + {}^{\bullet}AH \quad (5)$$

Firstly, H_2O_2 typically reacts rapidly with MPO-Fe(III) and generates a ferryl porphyrin **π** cation radical $\left(\text{MPO-Fe(IV)} = O^{\bullet+}\pi_{\text{Por}}\right)$ intermediate named Compound I (Eq. (1)) [11,12]. Compound I is capable of oxidizing either Cl^- through a $2e^-$ transition, generating MPO-Fe(III) and HOCl (Eq. (2)) or it can oxidize multiple organic and inorganic molecules (AH_2) by two successive sequential $1e^-$ transitions generating their corresponding free radicals ($^{\bullet}AH$) and the peroxidase intermediates Compound II (MPO-Fe(IV) = O) and MPO-Fe(III), respectively (Eqs. (3) and (5)) [11–15]. Compound II is a longer lasting intermediate whose

decay to MPO-Fe(III) is considered to be the rate-limiting step during steady-state catalysis [12,15]. In some cases, the chlorinating activity of MPO can be disturbed through the formation of Compound I* that can be characterized by the electron hopping from the porphyrin ring site to a specific amino acid residue located near the heme molecule (Eq. (4)), and displays electron-acceptor properties [16–18]. Acceleration in Compound II formation and decay has been examined using series of organic and inorganic substrates as well as physiological reductants like nitric oxide and superoxide [11–14,19,20]. Chloride binds close enough to the heme iron of the peroxidase to influence both its reduction potential and binding affinity to small molecules, such as NO and superoxide, when these molecules bind to the heme center of the enzyme [21–23].

Mesna, (2-mercaptoethanesulfonic acid sodium salt), is an adjuvant drug utilized to reduce the risk of hemorrhagic cystitis in patients receiving treatment with chemotherapy such as isofamide or cyclophosphoamide, in general oxazaphosphorine chemotherapy [24,25]. Mesna is a cytoprotectant, which works by binding to the break down products of ifosfamide or cyclophosphoamide through a Michael addition to form a less harmful substance and reduce the risk of hemorrhage [24,25]. It is administered either orally or intravenously (IV) injected, most notably at the same time as the chemotherapy treatment [26,27]. When given orally, it's at 40% of the ifosfamide (1.2 g/m^2) dose at 2 and 6 h after each dose of ifosfamide or IV at 20% of the ifosfamide (1.2 g/m^2) dose once at the time of ifosfamide administration and 20% of the ifosfamide dose 4 and 8 h after each dose of ifosfamide, or as a single injection followed by 2 oral doses [26,27]. Alternatively, 10% of the dose can be given before the ifosfamide infusion and the remainder continued during and for 12–24 h after the ifosfamide infusion has stopped [26,27].

Myeloperoxidase-mediated reactive oxidants promote oxidative tissue damage in a variety of inflammatory diseases, ranging from various cancers, cardiovascular disorders and infertility [4,9,28]. Mesna, an agent known for its antioxidant properties and reducing the undesired side effects of chemotherapeutics, displays minimum to no side effects. Despite the beneficiary effects of mesna, which is reducing side effects of chemotherapy [24,25], limited information is known about its influence on regulating the activity and function of inflammatory enzymes such as MPO. In conjunction, many studies have displayed the key role mesna plays in eliminating harmful toxins from the body [29–33]. However, the exact mechanism through which mesna inhibits MPO remains to be explored. In this report, we utilize a combination of optical absorbance and rapid kinetics measurements to show that mesna is an effective inhibitor of MPO.

2. Results

2.1. Rapid kinetic measurements

To examine the kinetics of interaction between mesna and MPO compounds I and II, we first utilized diode array stopped-flow spectroscopy to assess the influence of mesna on MPO intermediates' build-up (amount formed), duration (stability), and decay, as these events occur during steady-state catalysis. The experiments were initiated at 10 °C by rapid mixing a fixed amount of a buffer solution supplemented with fixed amount of MPO-Fe(III) (~1.0 μM) in the absence and presence of increasing concentrations of mesna (0, 10, 50, and 500

μM; final) with a same volume of buffer solution supplemented with physiological concentrations of H_2O_2 (20 μM final). As previously reported, MPO-Fe (III) as isolated display a Soret absorbance peak centered at 430 nm and visible bands at 573, 630, and 694 nm. Addition of H_2O_2 to MPO-Fe(III) in the absence of co-substrates leads to the accumulation of compound II via rapid initial formation of compound I, and subsequent spontaneous single electron heme reduction. Compound II, the rate-limiting intermediate in the peroxidase cycle, decays slowly back to MPO-Fe (III). Fig. 1a shows the buildup of MPO compound I that occurs in the first 0.009 s of initiating the reaction which was characterized by a significant decrease in the extinction coefficient of the Soret absorbance peak and a shift from 432 to 428 nm. Fig. 1b shows its conversion to compound II that occurs in the next 20 s and displays a Soret absorbance peak at 450 nm and visible bands centered at 600 and 628 nm. This transient intermediate is relatively stable and converts very slowly to the ferric state. Fig. 1c shows the conversion of Compound II to MPO-Fe(III) that occurs in 800 s, this slow conversion still remains incomplete and requires more time for completion.

At all concentrations recorded, the addition of mesna to MPO-Fe(III) (~2 μM) showed that there was a very slow decrease (~5%) in Soret band region over two hours of incubation indicating that the affinity of mesna is very low towards MPO alone. Similarly, the addition of mesna had no effect on MPO Compound I formation. However, the addition of increasing concentrations of mesna to reaction mixtures results in dramatic effects on the MPO Compound II accumulation, rate of formation, duration, and decay rate, as assessed by multiple wavelength stopped-flow spectroscopy (Fig. 1). At low mesna concentrations, our results showed that it was readily used as a single electron substrate by Compound I and II, as indicated by the dramatic increase of MPO Compound II accumulation rate and its decay to MPO-Fe(III), respectively. As shown in Fig. 1d-i, the presence of mesna (<10 μM; final), the rate of Compound II accumulation was enhanced and increased in a concentration-dependent manner. In addition, it had a variable effect on the duration and amplitude of steady-state concentrations of Compound II that developed following H_2O_2 addition.

In the presence of higher mesna concentrations (>10 μM; final), the buildup of the peak at 450 nm cannot been seen, instead an initial rapid decrease in absorbance at 430 nm was followed by immediate decay to MPO-Fe(III), within seconds (Fig. 1j-l). This kinetic behavior is consistent with the formation of new Compound I like (Compound I*) intermediate that displays a characteristic spectrum similar to that of Compound I [16–18]. This new intermediate exhibits a low extinction coefficient with a Soret absorption peak at 428 nm and two resolved visible peaks centered at 570 and 625 nm (Fig. 1j-l). Compound I* is unstable and converts immediately to MPO-Fe(III) (Fig. 1j-l).

2.1.1. Effect of mesna on the formation, duration, and decay of MPO Compound II formation during steady-state catalysis—

To take a closer look at the reaction mechanism of the metabolism of mesna by MPO, we next investigated the influence of mesna on the kinetics of MPO Compound I, Compound I*, and Compound II and buildup, duration, and decay using single wavelength stopped-flow methods. Experiments were carried out by following the absorbance changes at 430 and 450 nm both in the absence and presence of Cl^-. In the absence of mesna, monitoring the reaction at 450 nm there was a

rapid increase in absorbance which reached a maximum intensity in less than 3 s, and then decayed slowly over a period of approximately 1000 s when a solution of 1 μM was rapidly mixed with 20 μM H_2O_2 (Fig. 2). The time course for each step was best fitted to a single exponential function with values of k_1 and k_2 of 1.30 and 0.00042 s^{-1}, respectively. The increase in absorbance at the start of the reaction can be attributed to the formation of MPO Compound II while the subsequent decrease in absorbance that took place over the next 1000 s can be attributed to the decay of this intermediate to MPO-Fe (III). In the presence of 5 μM mesna, again both the initial increase in absorbance and the decay were fitted to a single exponential function with a rate constant of 1.5 s^{-1} and 0.09 s^{-1} to the first and second phase, respectively, suggesting that mesna serves as a single electron substrate for both Compounds I and II. Increasing mesna concentrations not only signifies an increase in the buildup and the decay of Compound II but it decreases the amplitude, which is reflective of a decrease in the accumulation of Compound II (Fig. 2). The pseudo first order rate of both phases increased linearly when plotted as a function of mesna concentration, yielding second-order rate constants of 8.5 $\mu M^{-1}s^{-1}$ and 0.012 $\mu M^{-1}s^{-1}$ for the first and second phases, respectively (Fig. 3a-b). In both cases, the plots intersected the Y-axis near the rate in the absence of mesna, or at the origin, indicating that the transient intermediates and subsequent formed are essentially irreversible.

In the absence of mesna, when the reaction was monitored at 430 nm, the initial decrease in absorbance that occurs in the first millisecond was attributed to the formation of MPO Compound I and the subsequent slow increase in absorbance was attributed to the slow decay of Compound II to MPO-Fe(III). In the presence of increasing concentrations of mesna, it generates a more complex system by generation of Compound I (at lower concentrations of mesna) and subsequent conversion to Compound I* (at higher concentration of mesna) where both compounds decay immediately to MPO-Fe(III). Under these circumstances Compound I* seems likely to be more stable than Compound I, therefore it accumulated during steady-state catalysis. As summarized in Fig. 4, the addition of increasing concentrations of mesna to MPO reaction yields dramatic effects on the decay of the steady-state accumulation rates. The buildup rate constant of the formation of Compound I and amount of steady-state accumulation did not change by increasing mesna concentrations as judged by the same amplitude throughout (Fig. 5A).

Single-wavelength stopped-flow measurements were performed to determine the critical concentration when mesna switches its role from mediating destabilization of Compound I to Compound I*. The increase in absorbance followed at 430 nm was fitted to a one-exponential function, and the observed rate constant of Compound II/I* decay to MPO–Fe(III) was plotted as a function of mesna concentration. As shown in Fig. 5B, the rate of decay increased with increasing mesna concentration, with an inflection point at ~66 μM mesna to a slower rate. The inflection point shows the conversion of Compound II to MPO-Fe(III) to Compound I* which subsequently decays to MPO-Fe(III) through the formation of Compound II. The second order rate constants calculated from the slopes of the two phases, were determined to be 0.0056 and 0.0012 s^{-1} μM^{-1}, respectively (Fig. 5b).

2.1.2. The influence of Cl^- on the kinetics of MPO compound II build-up, duration, and decay during steady-state catalysis—We next investigated whether

the physiologically relevant plasma level of Cl^- in the reaction changed MPO intermediate distributions during steady-state catalysis. Experiments were performed in the absence and presence of mesna at increasing concentrations (25–350 μM). Addition of H_2O_2 to MPO solution in the presence of 100 mM Cl^- caused rapid small decreases in absorbance at 430 nm followed by instant recovery (Fig. 6) under these circumstances the enzyme generates HOCl. When the same reactions were repeated in the presence of 50 μM mesna there was a rapid decrease in absorbance indicating that mesna competes with Cl^- and switches the reaction from a two electron oxidation to a single electron oxidation pathway making the spectral changes similar regardless of the presence or absence of Cl^-. Increasing mesna concentration did not affect the rate of MPO Compound I/I* formation, but increased the amplitude of Compound I/I* and also increased the rate of complex decay rate (Fig. 7). Since high mesna concentrations were used the subsequent increase in absorbance was attributed to formation of Compound I* through the formation of Compound I. While the decay rate increased in a concentration-dependent and saturable manner as a function of increasing mesna concentrations. However, increasing mesna concentration had no effect on the rate of Compound I formation, intercept: 354 s^{-1} (Fig. 7).

2.1.3. Inactivation of MPO chlorinating by mesna—

We then investigated the consequences of mesna interaction with MPO-Fe(III) on the MPO chlorinating activity utilizing the taurine assay, a classical assay for MPO activity. Measurements were carried out by equilibrating the enzyme samples with different concentrations of mesna in the presence of a fixed amount of taurine, and the reactions were initiated by adding biologically relevant levels of H_2O_2 (10 μM final concentration) as described under “Experimental Procedures.” The effect of mesna concentration on the initial rate of MPO-Fe(III) catalysis is calculated and plotted as a function of mesna concentration. The observed decrease in the initial rate of MPO catalysis suggested that mesna promotes inhibition of MPO chlorinating activity. This was confirmed by stopped-flow kinetic studies, which demonstrated that the rate of Compound II reduction into MPO-Fe(III) was significantly increased in the presence of mesna. The percent of residual activity that was measured in the presence of increasing concentrations of mesna is shown in Fig. 8. Percent residual activity was obtained by calculating the rate from the linear portion of the generation of HOCl using taurine chloramine assay as previously described [34]. As shown in Fig. 8, mesna concentration (0–20 μM) affects the chlorinating activity of MPO at half concentration values (IC_{50}) calculated from the fit of the experimental curve to the means of the experimental data points was ~5 μM.

3. Discussion

Our current results not only highlight the potential role of mesna in inhibiting MPO but also make clear the potential inhibitory role of MPO Compound I*. At low mesna concentrations, mesna accelerates the conversion of MPO Compound I to Compound II and Compound II to MPO-Fe(III) suggesting that low mesna concentrations may function as a $1e^-$ substrate of both MPO Compounds I and II. However, at higher concentrations, mesna mediates the porphyrin-to-amino acid electron transfer allowing the formation of Compound I*, an intermediate that displays almost similar characteristic spectrum like MPO Compound

I. The electron transfer rate is dictated by the rate of the slowest electron transfer, which is the conversion of Compound I* to Compound II that remains much slower than the decay of Compound II to MPO-Fe(III). This potentially explains the decay of Compound I* to MPO-Fe(III) without the accumulation of Compound II. The ability of mesna to compete with plasma levels of Cl^- and switch the MPO-Fe(III) reaction from a $2e^-$ to a $1e^-$ oxidation pathway, inhibits the enzyme chlorinating activity and drives the enzyme to optimize its peroxidase activity accelerating the removal of the H_2O_2 from the MPO milieu. For instance, MPO serves as the major H_2O_2 scavenger in the human airway due to low levels of catalase [35], mesna could be potentially used as an inhibitor in a disease state like cystic fibrosis which causes an overproduction of MPO. The present studies support the notion that the formation of the Compound I* complex during steady-state catalysis is a fundamental feature of the kinetic reactions of MPO under these experimental conditions. A steady-state competition model that describes and incorporates our current findings is presented in Fig. 9. This working model consists of two major pathways: Pathway A, the classical peroxidase cycle; Pathway B, the ability of mesna to mediate the formation of MPO Compound I* and its decay to MPO-Fe(III). In Pathway A, MPO Compound I was the first intermediate that was formed through the reaction of MPO-Fe(III) with H_2O_2. Its formation is relatively fast and occurs independent of mesna with a first order rate constant of 225 s^{-1} at 10 °C in the absence of Cl^-, and 350 s^{-1} in the presence of Cl^- (Figs. 5A and 7A). MPO Compound I oxidizes Cl^-, the physiological substrate for MPO [36], in a $2e^-$ oxidation reaction leading to formation of MPO-Fe(III) and the generation of HOCl. The high rate of Cl^- catalysis was associated with undetectable Compound I buildup and minimal decrease in the Soret absorbance peak during the steady-state catalysis. The rate of compound II formation and stability depended on the concentration of mesna. In the absence of Cl^- and during turnover, Compound I is converted to Compound II both spontaneously by single electron leak (from endogenous electron donors) [14,19,37] and similarly however more rapidly in the presence of low concentrations of mesna. Thus, these findings are consistent with MPO Compound I and II being able to oxidize mesna through $1e^-$ pathway reactions in a concentration-dependent fashion, with a second-order rate constant of 0.032 and 0.006 $\mu M^{-1}s^{-1}$, respectively. Under these conditions formation of compound II occurs faster than its decay, therefore, the accumulation of Compound II can be seen. Increasing mesna concentration shortens Compound II duration (stability of Compound II) and decreases the amplitude (amount of Compound II formed).

In the presence of sub-saturated amounts of mesna, the transformation that is apparent from our diode array spectrophotometer represents a switch in subcycles, from pathway A to B (Fig. 9). In pathway B, mesna was able to constrain this reaction by accelerating the conversion of Compound I to MPO-Fe(III) through the formation of new transient intermediate, Compound I*. The presence of higher concentrations of mesna during MPO-Fe(III) catalysis and its peculiar binding to the enzyme heme pocket as a bulky molecule facilitates the instant porphyrin-to-amino acid electron transfer allowing the formation of Compound I*, and its decay consistent with the direct conversion to MPO-Fe(III) without the build-up of Compound II. When mesna concentrations were increased, the transition of the two subcycles of Compound II exhaustion was reflected by the inflection in the decay rate, with critical concentration of mesna at 66 μM (Fig. 5B). At lower concentrations, under

66 μM, mesna was capable of destabilizing Compound I/II, but did not lead to the formation of Compound I*. At higher mesna concentration and when Compound I* accumulates in the reaction milieu, the rate-limiting step becomes the decay of Compound I* to Compound II (Fig. 7B). Collectively, this indicates that the loss of MPO catalytic activity is due to the buildup of inactive intermediates, Compound II, and/or Compound I*. The formation of Compound I* has also been reported by others [16–18,38].

In the presence of Cl^- the rate of MPO compound II decay revealed saturable kinetics at levels of mesna above 400 μM. At higher concentrations, mesna binds to MPO-Fe(III) to form Compound I*. Thus, the first-order rate constant observed for saturating levels of mesna is 3.8 s^{-1} and should reflect the conversion of Compound I* to Compound II, which is independent of mesna concentration. Since the electron transfer rate is dictated by the rate of the slowest electron transfer, the decay of Compound I* to Compound II, our kinetic data suggests that this is reflective of the rate-limiting step in the catalytic cycle and occurs slower than the conversion of Compound II to MPO-Fe(III). Therefore, MPO Compound II is not accumulated hence Compound I* build up is seen. However, at lower mesna concentrations, the decay rate is best fitted to one exponential function, which is the average between the rate of formation and decay of Compound II, since the difference between the two rates is less than 5 fold. Compound II complex formation is intrinsic to catalysis and causes a majority of the enzyme to partition into catalase-like activity. Thus, inactivation of MPO and its duration can be controlled effectively by mesna supplementation.

Compound I* formation is due to the processes that involves electron transfer from the heme to a specific amino acid residue located near the heme molecule [16–18,38]. Electron transfer in redox reactions typically occur through: 1) a single-step electron tunneling where there is no modification in the redox state of the conductive medium: and 2) through multistep electron hopping transfer [39–41] where there is an alteration in the redox state thus the medium may be reversibly oxidized and reduced; importantly the electron which is being transferred by the electron donor is not necessarily the same as the electron being accepted by the electron acceptor [39–41]. Therefore, the electron transfer rate is dictated by the rate of the slowest step, which equals the slowest electron transfer. However, this is still much faster than the electron transfer of the single-step reaction [39]. In peroxidases, electron transfer into and out of the active sites takes place over long distances (> 10 Å) in concert with protons that hop to or from the active sites along amino acid side chains or along structured water channels [42]. Redox activation of these enzymes to produce heme-oxo intermediates of compounds I and II occurs with the movement of protons along these water channels or by amino acid side chains that connect the redox cofactor to the external aqueous environment [43].

A hypothetical model of the catalytic side of MPO that helps explain the electron transfer from the heme-to-adjacent amino acid residues either by direct hopping of the electron from the heme to the amino acids or by direct transfer utilizing a water network and the formation of Compound I* is shown in Fig. 10. The MPO heme is in a deep tapered cleft leaving the α and δ carbon-methyne bridges buried inside the protein while the γ and β carbon-methyne bridges far more exposed to solution [44–46]. Mesna binding within the SCN^- binding site (as shown in yellow, orange and blue in Fig. 10) or in the entrance in the distal heme pocket

not only disturbs the water molecules network (either by deletion, movements, and disturbance in the hydrogen bonding network), but also disrupts the geometry of the distal heme cavity that is associated with a drastic change in the visible spectrum of the prosthetic heme group. Waters (red spheres) fill in the pockets forming a continuous water network connecting the front side of the heme to the bulk of the solvent. Beside H336 that provides the proximal ligand to the iron with an iron-to-nitrogen distance of 2.19 Å, the distal H95 (orange) is the only histidine residue close to the heme Fe, which is exposed to the solvent where the extra electron is released. The distance between the heme Fe and H95 NE2 atom is 5.6 Å [44–46]. The heme and H95 are spaced by a water molecule which is 3.2 Å from the heme Fe and 2.7 Å to the H95 NE2 atom. In enzymes, histidine is known not to be involved in electron transfer hopping which involves the transfer of the electron in conjunction with other amino acid residues. Therefore, any electron exchange between the heme and H95 is likely mediated through the water network with eventual release of the electron directly into the solvent. On the other hand, H95 forms a hydrogen bond to this water and could act as a donor if the NE2 atom is protonated. It is well established that H95 is involved in MPO activity therefore its modification to histidinyl radicals could lead to the enzyme inactivation [47].

Other heme-adjacent aromatic amino residues that may also involve in the electron hopping include three Phe (green), one Trp (purple), and two Tyr (cyan). All Phe residues (F99, F366, and F407) are located at the front of the heme and partially exposed to the solvent in the pocket. The residues Trp and Tyr (W477, Y296, and Y334) are located behind the heme, buried in the middle of the protein, and not accessible by solvent [44–46]. Among these aromatic residues, F407 is the closest to the heme. The distance between the CZ atom of F407 and the CHB atom of the heme is ~4.6 Å. Of note, the heme ring and the aromatic ring of F407 are roughly parallel and in the same plane [44–46]. One possible mechanism of electron transfer is direct hopping of an electron from the heme to F407 due to their spatial closeness. The transferred electron may be directly released to the solvent in the pocket, or hop to the nearby F366 which is spatially closer than F407 to the bulk solvent. Another possibility is the electron being directly transferred to the solvent in the pocket and released into the solvent through the pathway of the continuous water network. The Trp and Tyr residues are unlikely to serve as electron acceptors because they are buried and distant from the heme, and in addition they are not exposed to any water networks which may lead to the solvent. Residue F99 is also distant from heme and therefore direct electron hopping from the heme to this residue is highly unlikely (Fig. 10). Electron transfer is essential and plays multiple roles, previously it was established that it is utilized to produce hemoproteins in situ drugs with antimalarial activity [48] and in addition plays an important role in protein folding [49].

Our current study utilizes concentrations of mesna that have been shown to induce biological effects in animal cells and tissues without any signs of toxicity or side effects [26,27,50]. Thus, the results of this study suggest a potential role for mesna as a therapeutic in the treatment of various inflammatory diseases. In addition, in animals, it has also been shown that mesna pretreatment not only has a protective effect against ethanol-induced gastric mucosal damage, but also significantly increases enzymatic (superoxide dismutase and catalase activity) and non-enzymatic (glutathione content) antioxidant machinery in the

gastric tissues [29]. In addition, mesna markedly reduced ethanol-induced lipid peroxidation, tumor necrosis factor-alpha, interleukin (IL)-1β, IL-6, and monocyte chemotactic protein-1 levels thus further reducing any potential injury to host tissue [29]. In a similar mechanism, mesna protects kidney tissue against ischemia/reperfusion injury induced by oxidative damage [51]. It has also shown that mesna significantly reduces colorectal tissue damage when administered orally or intraperitoneally by reducing oxidative stress, inflammation and apoptosis, likely through a mechanism that involves the inhibition of NF-κB and overexpression of iNOS [30]. Consistent with these results, we show that mesna is a potent inhibitor of MPO with an IC_{50} of 5 μM. Taking into consideration the very low toxicity and minimal side effects upon uptake of the high concentration of mesna, therefore, our current finding suggests mesna as a useful potential inhibitor of MPO. The inhibition of MPO by mesna is reversible and has not previously been implicated in macrophage dysfunction; however, given these complex relationships, the possibility could be investigated in context in future studies.

Mesna is also utilized by MPO as a one-electron substrate to generate a mesna radical, which then is dimmerized to di-mesna (Fig. 10). Di-mesna generation has been confirmed by MS-MS spectra and HPLC (data not shown), no sulfenic/sulfinic acid has been formed excluding the possibility that mesna potentially reacts with Compound I (or Compound I*) by direct oxygenation of SH group of mesna via oxygen-abstraction. Di-mesna, the inactive form of mesna, circulates in the body and collects in the kidney where it converts back to its original state, mesna, in the renal tubular epithelia by redox enzymes of the thioredoxin and glutaredoxin systems and also by non-enzymatic thiol-disulfide exchange with cysteine and glutathione [52–54]. The free sulfhydryl group in mesna is able to conjugate cytotoxic metabolites such as acrolein to eliminate its harmful toxicity [50]. Our current results help to further justify the instability of mesna versus di-mesna in plasma of patients who receive this as an adjuvant treatment during chemotherapy.

Collectively, the unique chemical and clinical properties of mesna have facilitated its repurpose as a new therapeutic option for use over the past five decades. The extraordinary chemo protection delivered by mesna and its metabolite di-mesna without impairment to the effectiveness of chemotherapy can be attributed to the redox equilibrium and differential transport of these compounds. This work has further magnified the application of mesna and its classification as a potent inhibitor of the chlorinating activity of MPO. Elevated MPO levels play an important role in several disorders such as atherosclerosis, gastric ulcers, cancer, and infertility [3–5]. Utilizing mesna as a potent inhibitor of MPO could improve patient outcome by decreasing lipid peroxidation and increasing the antioxidant capacity, therefore inhibiting the inflammatory responses.

4. Methods

4.1. Materials

Mesna used was of the highest purity grades obtained from Sigma Chemical Co. (St. Louis, MO).

4.2. Enzyme purification

Myeloperoxidase was initially purified from detergent extracts of human leukocytes by sequential lectin affinity and gel-filtration chromatography [55]. Trace levels of contaminating eosinophil peroxidase were then removed by passage over a sulfopropyl Sephadex column [56]. Purity of isolated MPO was established by demonstrating a Reinheitzal (RZ) value of > 0.85 (A_{430}/A_{280}), SDS–PAGE analysis with Coomassie blue staining, and gel tetramethylbenzidine peroxidase staining to confirm no contaminating eosinophil peroxidase activity. Enzyme concentration was determined spectrophotometrically utilizing extinction coefficients of 89,000 M^{-1} cm^{-1}/heme of MPO [57]. The concentration of the MPO dimer was calculated as half the indicated concentration of heme-like chromophore [58].

4.3. Absorbance measurements

Spectra were recorded with a Cary 100 Bio UV–visible spectrophotometer, at 25 °C, in phosphate buffer pH 7.4. Experiments were performed with a 1 mL cuvette containing MPO (1.0–1.2 μM) preincubated with increasing concentrations of mesna (6–200 μM), in the absence and presence of 100 mM Cl^-. Concentrated volumes of H_2O_2 solution were added to the sample cuvette (20 μM final), and absorbance changes were recorded from 300 to 700 nm.

4.4. Rapid kinetic measurements

The kinetic measurements of MPO Compound I and/or Compound II formation and decay in the absence and presence of different mesna and/or fixed Cl^- (100 mM) concentrations were performed using a dual syringe stopped-flow instrument obtained from Hi-Tech, Ltd. (Model SF-61). Experiments were initially performed under conditions identical to those recently reported for MPO and other related hemoproteins to facilitate comparison [59,60]. Measurements were carried out under an aerobic atmosphere at 10 °C following rapid mixing of equal volumes of an H_2O_2-containing buffer solution and a peroxidase solution that contained 100 mM Cl^- and/or different mesna concentrations. Reactions were monitored at both 430 and 450 nm. The time course of the absorbance change was fit to a single-exponential, ($Y = 1 - e\text{-}kt$), or a double-exponential ($Y = Ae\text{-}k_1t + Be\text{-}k_2t$) function as indicated. Signal-to-noise ratios for all kinetic analyses were improved by averaging at least six to eight individual traces.

In some experiments, the stopped-flow instrument was attached to a rapid scanning diode array device (Hi-Tech) designed to collect multiple numbers of complete spectra (200–700 nm) at specific time ranges. The detector was automatically calibrated relative to a holmium oxide filter, as it has spectral peaks at 360.8, 418.5, 446.0, 453.4, 460.4, 536.4, and 637.5 nm, which were used by the software to correctly align pixel positions with wavelength. Rapid scanning experiments involved mixing solutions of peroxidase (1–2 μM) pre-incubated with 100 mM Cl^- in the absence or in the presence of increasing (5–200 μM) mesna concentrations with buffer solutions containing 40 μM H_2O_2, at 10 °C.

4.5. Taurine chloramine assay

Hypochlorous acid levels were determined as previously described [34] with minor modifications. Briefly, experiments were performed in 200 μL final volume containing 50 mM phosphate buffer, pH 7.4, and 10 mM taurine using a 96-well plate reader (Spectra Max 190; Molecular Devices, Sunnyvale, FL, USA). Reactions were initiated by adding H_2O_2 (20 μM) to a solution containing MPO (40 nM) and Cl^- (100 mM) in the absence and presence of various concentrations of mesna. The percentage of residual activity was calculated from the initial increase in absorbance at 650 nm.

4.6. Solutions preparation

A stock solution of mesna was dissolved in H_2O and then diluted to the required concentration with phosphate buffer (pH = 7.4).

Acknowledgments

☆ This work was supported by a grant from the National Institutes of Health (RO1 HL066367, H.M.A-S.).

Abbreviations:

Cl^-	Chloride
MPO	Myeloperoxidase
H_2O_2	Hydrogen peroxide
e^-	Electron

References

[1]. Nauseef WM, Malech HL, Analysis of the peptide subunits of human neutrophil myeloperoxidase, Blood 67 (5) (1986) 1504–1507. [PubMed: 3008892]

[2]. Nauseef WM, Cogley M, McCormick S, Effect of the R569W missense mutation on the biosynthesis of myeloperoxidase, J. Biol. Chem 271 (16) (1996) 9546–9549. [PubMed: 8621627]

[3]. Davies MJ, et al., Mammalian heme peroxidases: from molecular mechanisms to health implications, Antioxid. Redox Signal 10 (7) (2008) 1199–1234. [PubMed: 18331199]

[4]. Nicholls SJ, Hazen SL, Myeloperoxidase and cardiovascular disease, Arterioscler. Thromb. Vasc. Biol 25 (6) (2005) 1102–1111. [PubMed: 15790935]

[5]. Podrez EA, Abu-Soud HM, Hazen SL, Myeloperoxidase-generated oxidants and atherosclerosis, Free Radic. Biol. Med 28 (12) (2000) 1717–1725. [PubMed: 10946213]

[6]. Undurti A, et al., Modification of high density lipoprotein by myeloperoxidase generates a pro-inflammatory particle, J. Biol. Chem 284 (45) (2009) 30825–30835. [PubMed: 19726691]

[7]. Heinecke JW, The role of myeloperoxidase in HDL oxidation and atherogenesis, Curr. Atheroscler. Rep 9 (4) (2007) 249–251. [PubMed: 18173946]

[8]. Nicholls SJ, Hazen SL, Myeloperoxidase, modified lipoproteins, and atherogenesis, J. Lipid Res (50 Suppl) (2009) S346–S351. [PubMed: 19091698]

[9]. Fletcher NM, et al., Myeloperoxidase and free iron levels: potential biomarkers for early detection and prognosis of ovarian cancer, Cancer Biomark. 10 (6) (2011) 267–275. [PubMed: 22820082]

[10]. Maitra D, et al., Myeloperoxidase acts as a source of free iron during steady-state catalysis by a feedback inhibitory pathway, Free Radic. Biol. Med 63 (2013) 90–98. [PubMed: 23624305]

[11]. Hurst JKE, Everse J, Everse KE, Grisham MB, Peroxidases in Chemistry and Biology, 1 CRC Press, Boca Raton, FL, 1991, pp. 37–62.

[12]. Kettle AJ, Winterbourn CC, Myeloperoxidase: a key regulator of neutrophil oxidant production, Redox Rep. 3 (1) (1997) 3–15. [PubMed: 27414766]

[13]. Marquez LA, Huang JT, Dunford HB, Spectral and kinetic studies on the formation of myeloperoxidase compounds I and II: roles of hydrogen peroxide and superoxide, Biochemistry 33 (6) (1994) 1447–1454. [PubMed: 8312264]

[14]. Marquez LA, Dunford HB, Van Wart H, Kinetic studies on the reaction of compound II of myeloperoxidase with ascorbic acid. Role of ascorbic acid in myeloperoxidase junction, J. Biol. Chem 265 (10) (1990) 5666–5670. [PubMed: 2156823]

[15]. Furtmuller PG, et al., Spectral and kinetic studies on the formation of eosinophil peroxidase compound I and its reaction with halides and thiocyanate, Biochemistry 39 (50) (2000) 15578–15584. [PubMed: 11112545]

[16]. Gau J, et al., Flavonoids as promoters of the (pseudo-)halogenating activity of lactoperoxidase and myeloperoxidase, Free Radic. Biol. Med 97 (2016) 307–319. [PubMed: 27350402]

[17]. Bafort F, et al., Mode of action of lactoperoxidase as related to its antimicrobial activity: a review, Enzyme Res. 2014 (2014) 517164. [PubMed: 25309750]

[18]. Jantschko W, et al., Reaction of ferrous lactoperoxidase with hydrogen peroxide and dioxygen: an anaerobic stopped-flow study, Arch. Biochem. Biophys 434 (1) (2005) 51–59. [PubMed: 15629108]

[19]. Abu-Soud HM, Hazen SL, Nitric oxide is a physiological substrate for mammalian peroxidases, J. Biol. Chem 275 (48) (2000) 37524–37532. [PubMed: 11090610]

[20]. Abu-Soud HM, et al., Peroxidases inhibit nitric oxide (NO) dependent bronchodilation: development of a model describing NO-peroxidase interactions, Biochemistry 40 (39) (2001) 11866–11875. [PubMed: 11570887]

[21]. Winterbourn CC, Kettle AJ, Reactions of superoxide with myeloperoxidase and its products, Jpn. J. Infect. Dis 57 (5) (2004) S31–S33.

[22]. Abu-Soud HM, Hazen SL, Nitric oxide modulates the catalytic activity of myeloperoxidase, J. Biol. Chem 275 (8) (2000) 5425–5430. [PubMed: 10681518]

[23]. Proteasa G, et al., Kinetic evidence supports the existence of two halide binding sites that have a distinct impact on the heme iron microenvironment in myeloperoxidase, Biochemistry 46 (2) (2007) 398–405. [PubMed: 17209550]

[24]. Andriole GL, et al., The efficacy of mesna (2-mercaptoethane sodium sulfonate) as a uroprotectant in patients with hemorrhagic cystitis receiving further oxazaphosphorine chemotherapy, J. Clin. Oncol 5 (5) (1987) 799–803. [PubMed: 3106585]

[25]. Sakurai M, et al., The protective effect of 2-mercapto-ethane sulfonate (MESNA) on hemorrhagic cystitis induced by high-dose ifosfamide treatment tested by a randomized crossover trial, Jpn. J. Clin. Oncol 16 (2) (1986) 153–156. [PubMed: 3090314]

[26]. Goren MP, Oral administration of mesna with ifosfamide, Semin. Oncol 23 (3 Suppl 6) (1996) S91–S96.

[27]. Goren MP, Oral mesna: a review, Semin. Oncol 19 (6 Suppl 12) (1992) S65–S71.

[28]. Shaeib F, et al., The impact of myeloperoxidase and activated macrophages on metaphase II mouse oocyte quality, PLoS One 11 (3) (2016) e0151160. [PubMed: 26982351]

[29]. Amirshahrokhi K, Khalili AR, Gastroprotective effect of 2-mercaptoethane sulfonate against acute gastric mucosal damage induced by ethanol, Int. Immunopharmacol 34 (2016) 183–188. [PubMed: 26967742]

[30]. Triantafyllidis I, et al., Treatment with Mesna and n-3 polyunsaturated fatty acids ameliorates experimental ulcerative colitis in rats, Int. J. Exp. Pathol 96 (6) (2015) 433–443. [PubMed: 26852691]

[31]. Sener G, et al., 2-Mercaptoethane sulfonate (MESNA) protects against biliary obstruction-induced oxidative damage in rats, Hepatol. Res 35 (2) (2006) 140–146. [PubMed: 16584914]

[32]. Sener G, et al., Protective effect of MESNA (2-mercaptoethane sulfonate) against hepatic ischemia/reperfusion injury in rats, Surg. Today 35 (7) (2005) 575–580. [PubMed: 15976955]

[33]. Sener G, et al., Protective effects of MESNA (2-mercaptoethane sulphonate) against acetaminophen-induced hepatorenal oxidative damage in mice, J. Appl. Toxicol 25 (1) (2005) 20–29. [PubMed: 15669031]

[34]. Kettle AJ, Winterbourn CC, Assays for the chlorination activity of myeloperoxidase, Methods Enzymol. 233 (1994) 502–512. [PubMed: 8015486]

[35]. Erzurum SC, et al., In vivo antioxidant gene expression in human airway epithelium of normal individuals exposed to 100% O2, J. Appl. Physiol 75 (3) (1993) 1256–1262 (1985). [PubMed: 8226538]

[36]. Furtmuller PG, et al., The reactivity of myeloperoxidase compound I formed with hypochlorous acid, Redox Rep. 5 (4) (2000) 173–178. [PubMed: 10994870]

[37]. Kettle AJ, van Dalen CJ, Winterbourn CC, Peroxynitrite and myeloperoxidase leave the same footprint in protein nitration, Redox Rep. 3 (5–6) (1997) 257–258. [PubMed: 9754322]

[38]. Ma Z, Williamson HR, Davidson VL, A suicide mutation affecting proton transfers to high-valent hemes causes inactivation of MauG during catalysis, Biochemistry (2016).

[39]. Geng J, et al., Tryptophan-mediated charge-resonance stabilization in the bis-Fe (IV) redox state ofMauG, Proc. Natl. Acad. Sci. USA 110 (24) (2013) 9639–9644. [PubMed: 23720312]

[40]. Warren JJ, et al., Electron hopping through proteins, Coord. Chem. Rev 256 (21–22) (2012) 2478–2487. [PubMed: 23420049]

[41]. Georg S, et al., Distance-dependent electron transfer rate of immobilized redox proteins: a statistical physics approach, Phys. Rev. E Stat. Nonlinear Soft Matter Phys 81 (4 Pt 2) (2010) 046101.

[42]. Reece SY, et al., Proton-coupled electron transfer: the mechanistic underpinning for radical transport and catalysis in biology, Philos. Trans. R. Soc. Lond. B Biol. Sci 361 (1472) (2006) 1351–1364. [PubMed: 16873123]

[43]. Pond AE, Sono MLP, Goodin DB, Dawson JH, edox enzymes: correlation of three-dimensional structure and mechanism for heme-containing oxygenases and peroxidases, in: Balzani V. (Ed.), Electron Transfer In Chemistry, 3.1.4 Wiley-VCH, Weinheim, Germany, 2001, pp. 56–104.

[44]. Blair-Johnson M, Fiedler T, Fenna R, Human myeloperoxidase: structure of a cyanide complex and its interaction with bromide and thiocyanate substrates at 1.9 A resolution, Biochemistry 40 (46) (2001) 13990–13997. [PubMed: 11705390]

[45]. Fiedler TJ, Davey CA, Fenna RE, X-ray crystal structure and characterization of halide-binding sites of human myeloperoxidase at 1.8 A resolution, J. Biol. Chem 275 (16) (2000) 11964–11971. [PubMed: 10766826]

[46]. Davey CA, Fenna RE, 2.3 A resolution X-ray crystal structure of the bisubstrate analogue inhibitor salicylhydroxamic acid bound to human myeloperoxidase: a model for a prereaction complex with hydrogen peroxide, Biochemistry 35 (33) (1996) 10967–10973. [PubMed: 8718890]

[47]. Kobayashi M, Tanaka T, Usui T, Inactivation of lysosomal enzymes by the respiratory burst of polymorphonuclear leukocytes. Possible involvement of myeloperoxidase-H2O2-halide system, J. Lab. Clin. Med 100 (6) (1982) 896–907. [PubMed: 6292313]

[48]. Meunier B, Robert A, Heme as trigger and target for trioxane-containing antimalarial drugs, Acc. Chem. Res 43 (11) (2010) 1444–1451. [PubMed: 20804120]

[49]. Pascher T, et al., Protein folding triggered by electron transfer, Science 271 (5255) (1996) 1558–1560. [PubMed: 8599112]

[50]. Shaw IC, Graham MI, Mesna–a short review, Cancer Treat. Rev 14 (2) (1987) 67–86. [PubMed: 3119211]

[51]. Kabasakal L, et al., Mesna (2-mercaptoethane sulfonate) prevents ischemia/reperfusion induced renal oxidative damage in rats, Life Sci. 75 (19) (2004) 2329–2340. [PubMed: 15350830]

[52]. Leeuwenkamp OR, et al., Reaction kinetics of cisplatin and its monoaquated species with the modulating agents (di)mesna and thiosulphate, Eur. J. Cancer 27 (10) (1991) 1243–1247. [PubMed: 1835593]

[53]. Nishikawa A, Morse MA, Chung FL, Inhibitory effects of 2-mercaptoethane sulfonate and 6-phenylhexyl isothiocyanate on urinary bladder tumorigenesis in rats induced by N-butyl-N-(4-hydroxybutyl)nitrosamine, Cancer Lett. 193 (1) (2003) 11–16. [PubMed: 12691818]

[54]. Lahdetie J, Raty R, Sorsa M, Interaction of Mesna (2-mercaptoethane sulfonate) with the mutagenicity of cyclophosphamide invitro and invivo, Mutat. Res 245 (1) (1990) 27–32. [PubMed: 2118231]

[55]. Rakita RM, Michel BR, Rosen H, Differential inactivation of Escherichia coli membrane dehydrogenases by a myeloperoxidase-mediated antimicrobial system, Biochemistry 29 (4) (1990) 1075–1080. [PubMed: 1692736]

[56]. Wever R, Plat H, Hamers MN, Human eosinophil peroxidase: a novel isolation procedure, spectral properties and chlorinating activity, FEBS Lett. 123 (2) (1981) 327–331. [PubMed: 6262111]

[57]. Agner K, Acta Chem. Scand 17 (1963) S332–S338.

[58]. Andrews PC, Krinsky NI, Akinetic analysis of the interaction of human myeloperoxidase with hydrogen peroxide, chloride ions, and protons, J. Biol. Chem 257 (22) (1982) 13240–13245. [PubMed: 6292181]

[59]. Galijasevic S, Abdulhamid I, Abu-Soud HM, Potential role of tryptophan and chloride in the inhibition of human myeloperoxidase, Free Radic. Biol. Med 44 (8) (2008) 1570–1577. [PubMed: 18279680]

[60]. Galijasevic S, Abdulhamid I, Abu-Soud HM, Melatonin is a potent inhibitor for myeloperoxidase, Biochemistry 47 (8) (2008) 2668–2677. [PubMed: 18237195]

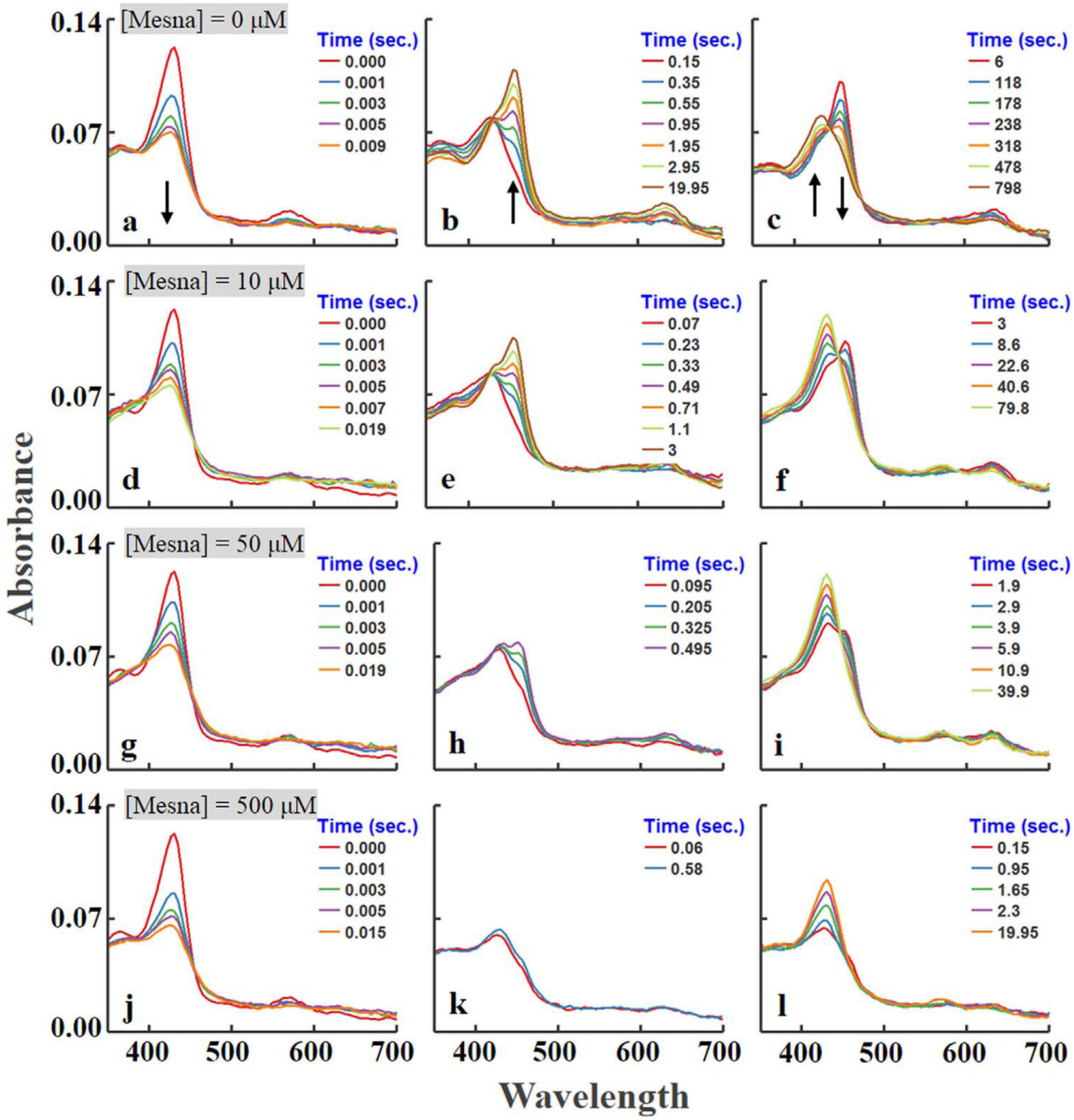

Fig. 1.

Diode array rapid scanning spectra for the intermediates and for the reaction of increasing concentrations of mesna with MPO-Fe(III) at three sequential time frames. Experiments were carried out by rapid mixing a solution containing sodium phosphate buffer (200 mM, pH 7.4) supplemented with 1 μm (final) MPO-Fe(III) and increasing concentrations of mesna (0, 10, 50, and 500, final) was rapidly mixed with an equal volume of buffer containing fixed concentrations of H_2O_2 (20 μM, final) at 10 °C. The final concentration of mesna in mixtures is indicated. Arrows indicate the direction of spectral change over time as

each intermediate advanced to the next. These data are representative of three independent experiments.

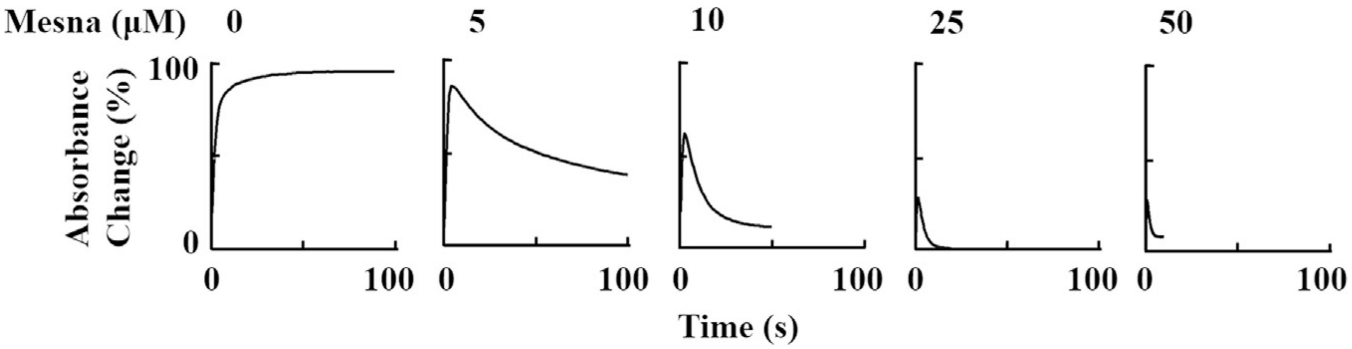

Fig. 2.

Stopped-flow analysis of the effect of increasing mesna concentrations on the formation, duration, and decay of MPO Compound II. A solution containing phosphate buffer (200 mM, pH 7.4) supplemented with 1–1.2 μM (final) MPO-Fe(III) and increasing concentrations of mesna (0, 5, 10, 25, 50, final) was rapidly mixed with an equal volume of buffer containing fixed concentrations of H_2O_2 (20 μM, final) at 10 °C. Formation, duration and decay of MPO Compound II were monitored at 450 nm. The final concentration of mesna in mixtures is indicated.

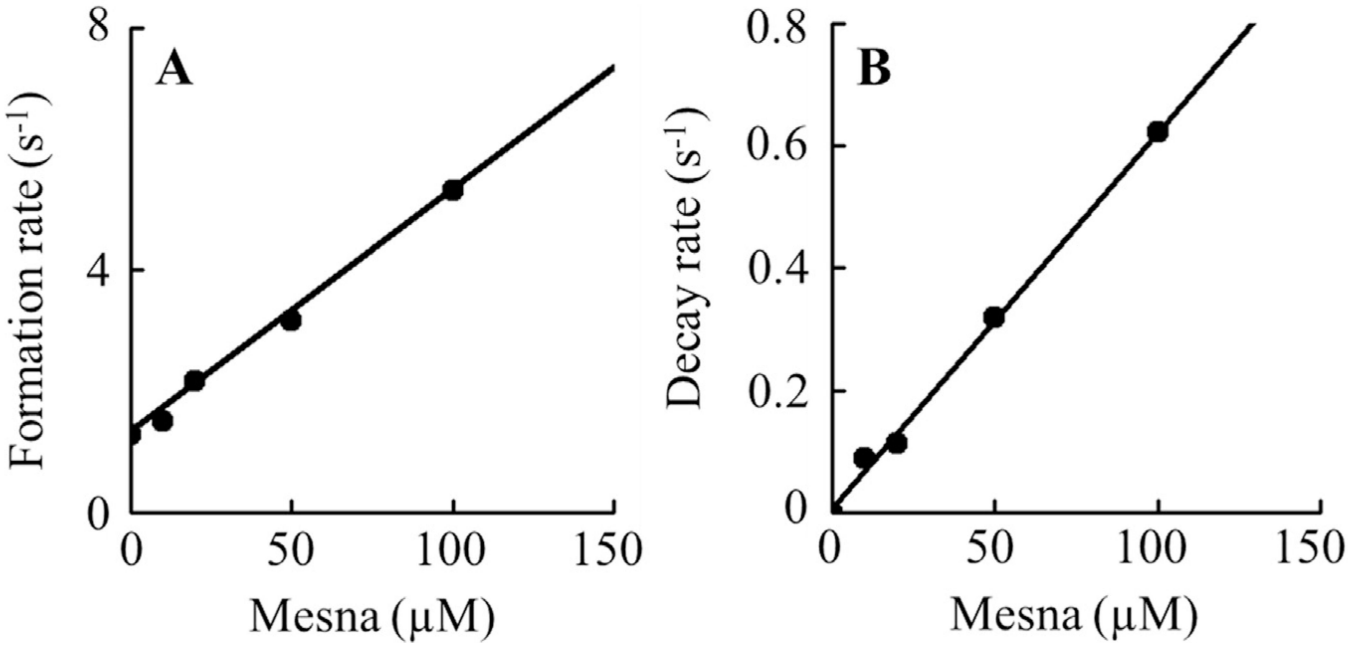

Fig. 3. Rate constants of the formation and decay of MPO Compound II intermediates as a function of mesna concentration.

Panel A, the observed rate constants of Compound II complex formation observed in Fig. 2 were plotted as a function of mesna concentration (R2 value was 0.9935 and slope was 0.03248). Data represents the mean of triplicate determinations from an experiment performed three times. Panel B, the rate constants for the decay of compound II complex (R2 value was 0.9962 and slope was 0.00615), for the same reaction monitored at 450 nm as a function of mesna concentration. These data are representative of three independent experiments and the standard error for each individual rate constant has been estimated to be less than 6%.

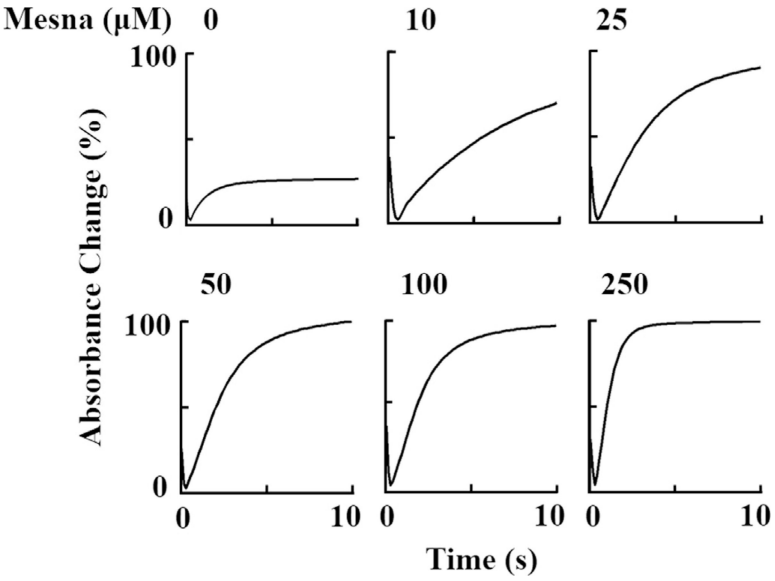

Fig. 4.

Stopped-flow analysis of the effect of increasing mesna concentrations on the formation, duration, and decay of MPO Compounds I and II. A solution containing phosphate buffer (200 mM, pH 7.4) supplemented with 1–1.2 μM (final) MPO-Fe(III) and increasing concentrations of mesna (0, 10, 25, 50, 100, and 250 μM final) was rapidly mixed with an equal volume of buffer containing fixed concentrations of H_2O_2 (20 μM, final) at 10 °C. Formation, duration and decay of MPO Compounds I and II were monitored at 430 nm. The final concentration of mesna in mixtures is indicated.

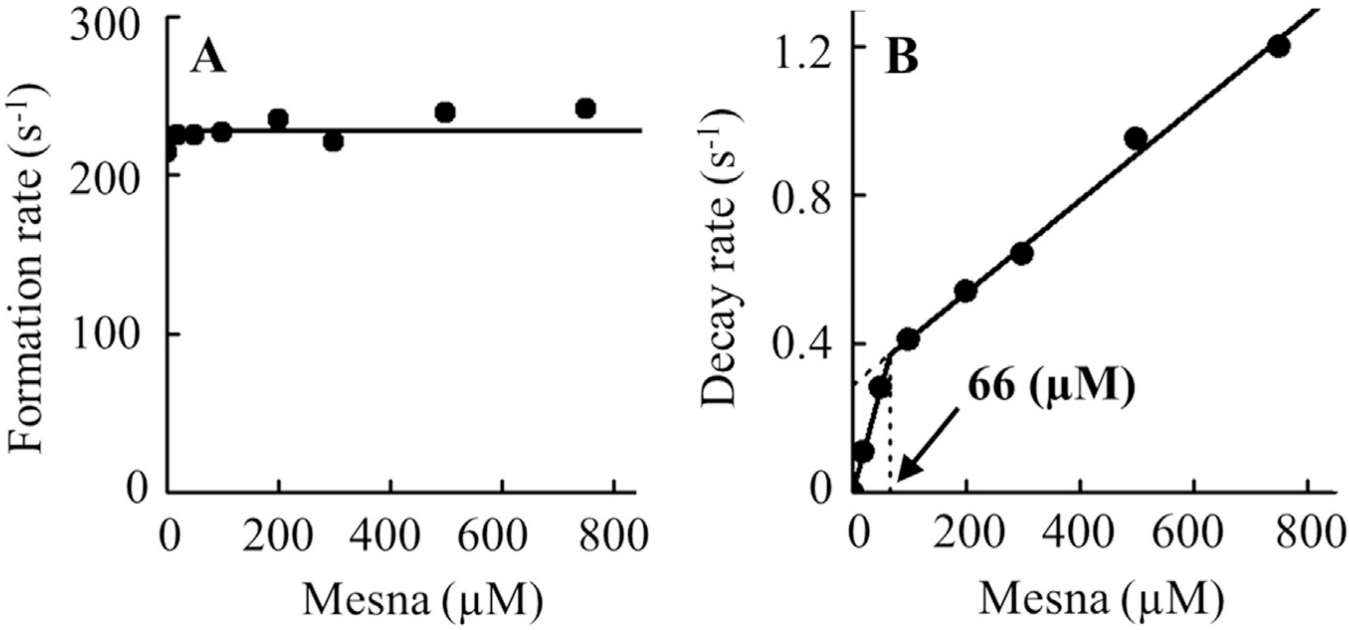

Fig. 5. Rate constants of the formation and decay of MPO Compounds I and II intermediates as a function of mesna concentration.

Panel A, the observed rate constants of Compound I complex formation observed in Fig. 4 were plotted as a function of mesna concentration. Data represents the mean of triplicate determinations from an experiment performed three times. Panel B, the rate constants for the decay of compound II complex (slope 1 was 0.03248 and slope 2 was 0.00615), for the same reaction monitored at 430 nm as a function of mesna concentration. These data are representative of three independent experiments and the standard error for each individual rate constant has been estimated to be less than 6%.

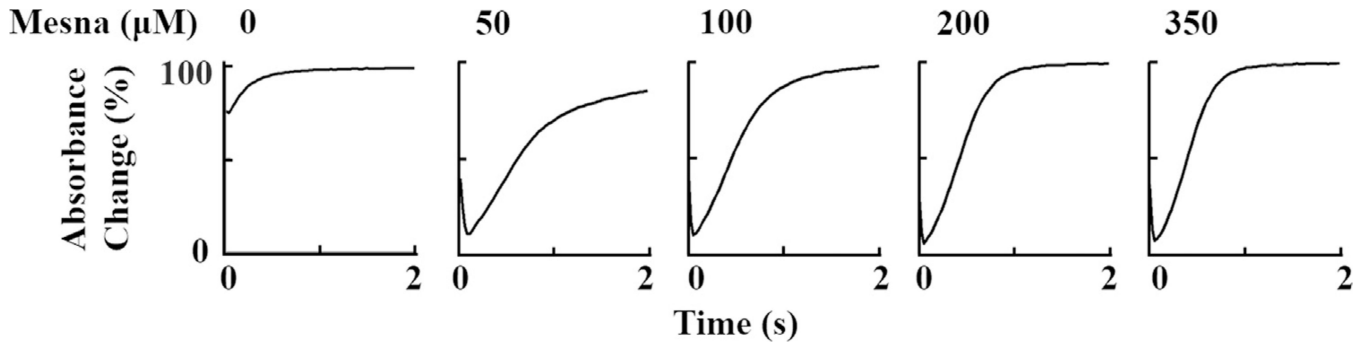

Fig. 6.

Rate constants of the formation and decay of MPO Compound I intermediates as a function of mesna concentration in the presence of Cl^-. A solution containing sodium phosphate buffer (200 mM, pH 7.4) and 100 mM Cl^- and supplemented with 1–1.2 μM (final) MPO-Fe(III) and increasing concentrations of mesna (0, 50, 100, 200, and 350 final) was rapidly mixed with an equal volume of buffer containing fixed concentrations of H_2O_2 (20 μM, final) at 10 °C. Formation, duration and decay of MPO Compound I were monitored at 430 nm. The final concentration of mesna in mixtures is indicated.

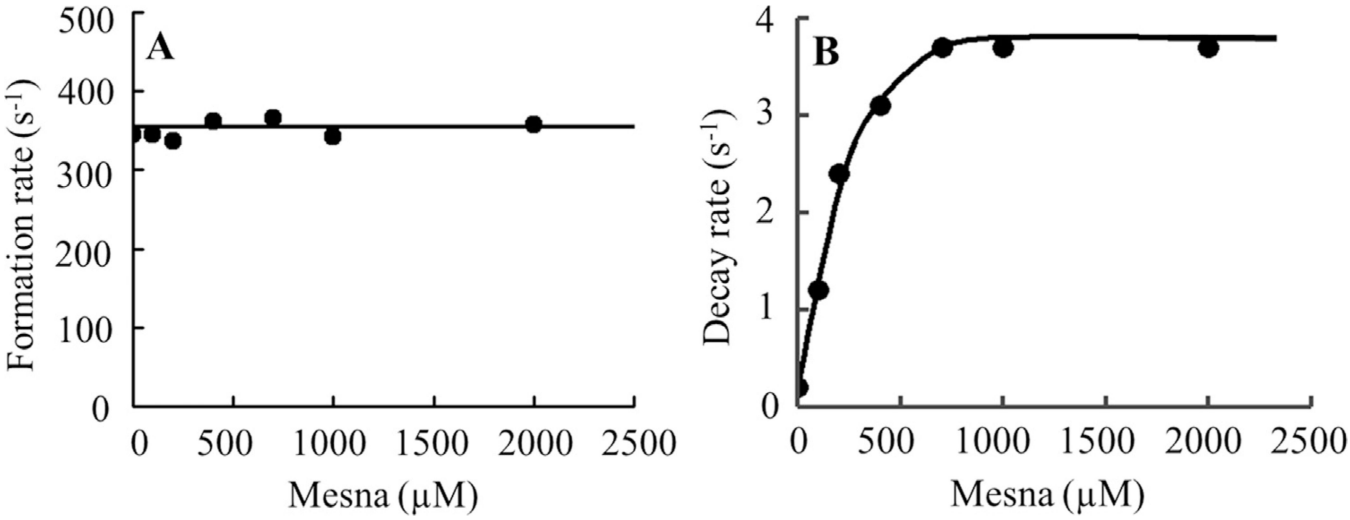

Fig. 7. Rate constants of the formation and decay of MPO Compound I intermediates as a function of mesna concentration.

Panel A, the observed rate constants of Compound I complex formation observed in Fig. 6 were plotted as a function of mesna concentration (R2 value was 0.1296 and slope was 0.0). Data represents the mean of triplicate determinations from an experiment performed three times. Panel B, the rate constants for the decay of compound II complex (slope was 0.01100), for the same reaction monitored at 430 nm as a function of mesna concentration. These data are representative of three independent experiments and the standard error for each individual rate constant has been estimated to be less than 6%.

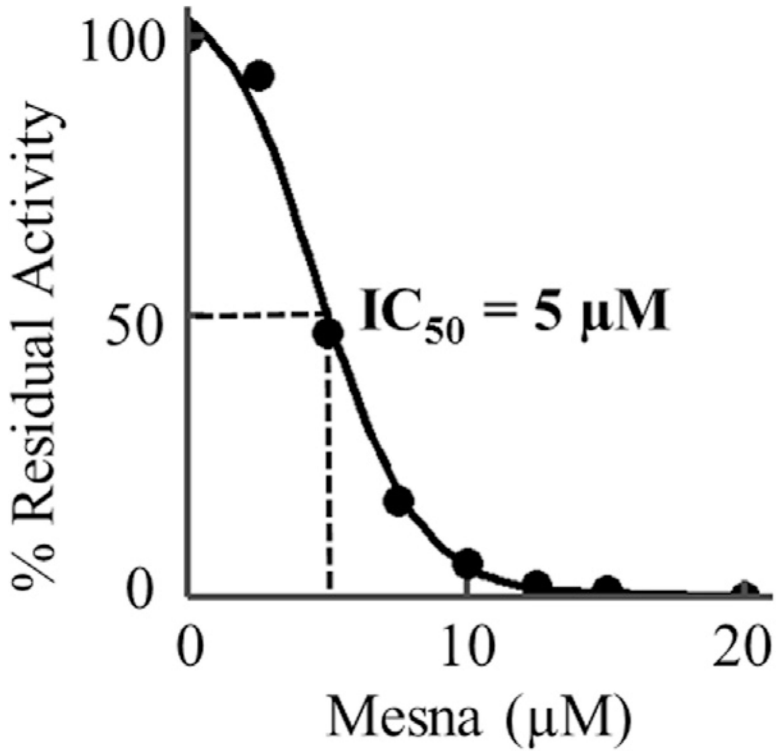

Fig. 8. A relatively low mesna concentrations Inactivate MPO chlorinating activity.

A, effect of Mesna on the chlorination activity of MPO was determined by the production of hypochlorous acid by 10 nM MPO in 10 mM phosphate buffer, pH 7.4, containing 140 mM sodium chloride, 5 mM taurine and increasing concentrations of mesna (0, 2.5, 5, 8, 10, 12.5, 15 and 20). Concentration of Mesna that inhibited production of hypochlorite by 50% (IC_{50}) was determined over a range of chloride concentrations. These data are representative of three independent experiments.

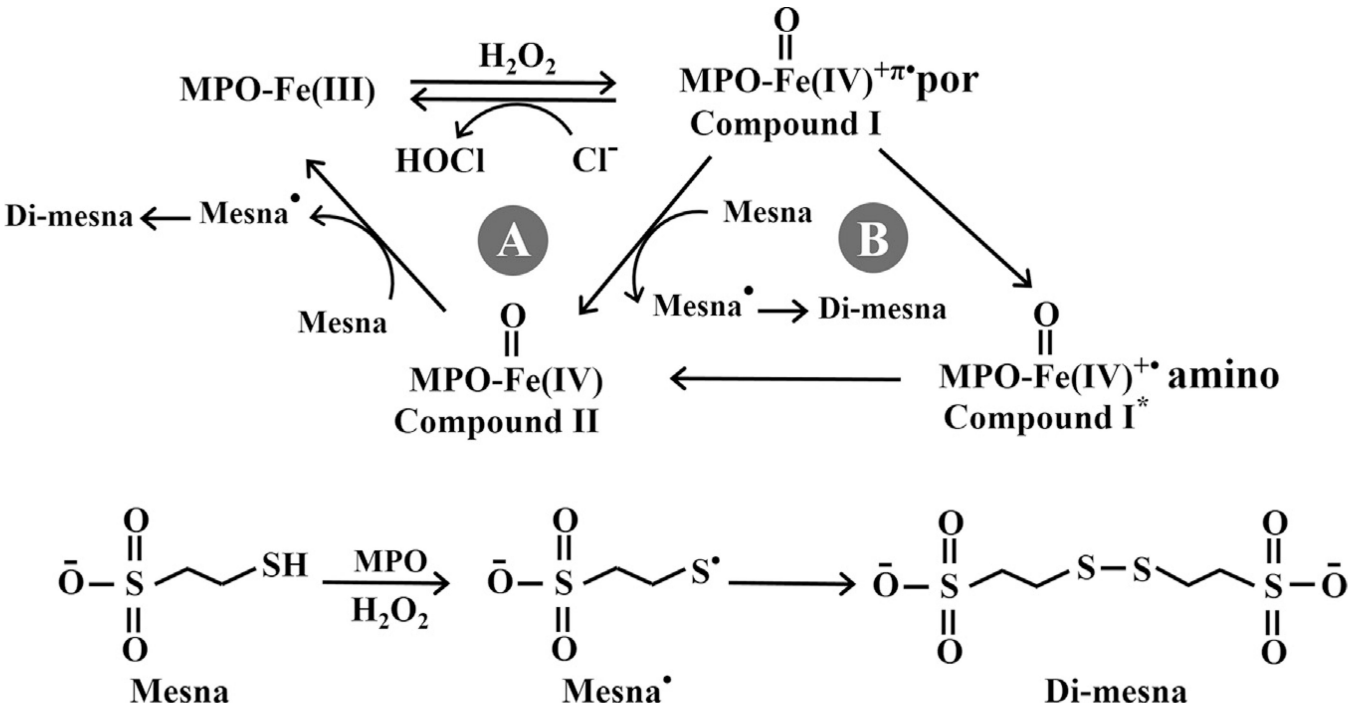

Fig. 9. Working kinetic model for mesna interactions with MPO.

Pathway A represents the typical classic peroxidase cycle. Pathway B shows the formation of MPO Compound I* and its conversion to MPO-Fe(III) through the formation of Compound II mediated by mesna.

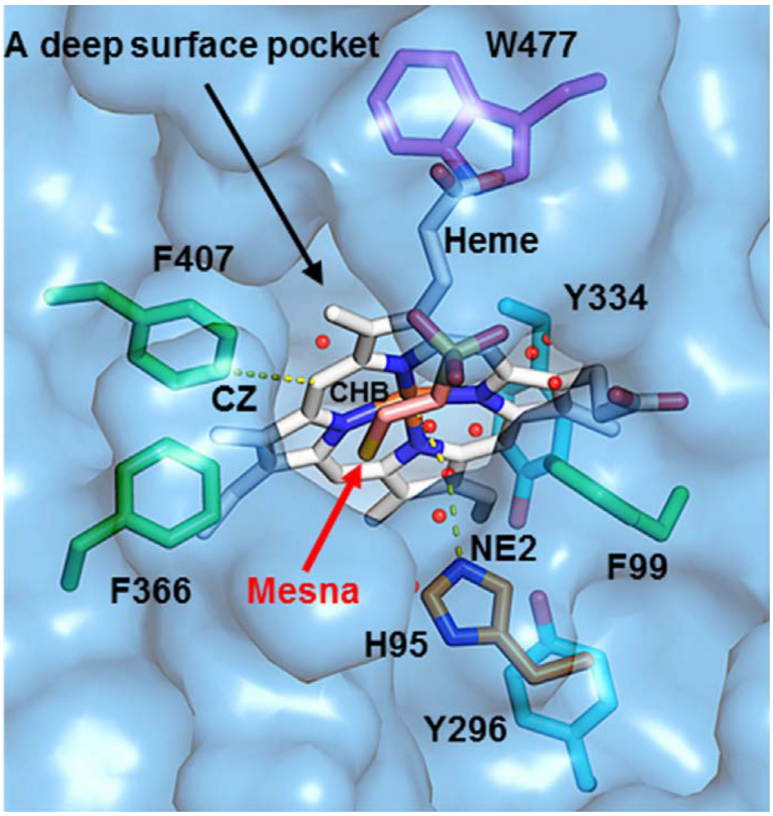

Fig. 10.

A hypothetical model of the catalytic side of MPO that helps explain how mesna could mediate the electron transfer and electron hopping from the heme-to-adjacent amino acid residues. The figure was made using the coordinates deposited in the Protein Data Bank (accession code 1DNU), using PyMOL (www.pymol.org).